

CHARACTERISATION OF EXTRAGALACTIC SOURCE POSITIONS THAT DEFINE THE CELESTIAL REFERENCE FRAME

C. Gattano¹ and P. Charlot¹

Abstract. We investigated the astrometric position variations of the most observed sources in astrometric and geodetic VLBI, with the goal of characterizing such variations. In a first stage, we aimed at categorizing individually the source positions. Are they stable enough under the VLBI astrometric accuracy to materialize ultra-accurate fiducial marks on the sky. In a second stage, our goal was to determine whether there are any preferred directions in those source position variations. Our result favor source-dependent systematic variability that affect the position stability. Additionally, it was also found that the source position variations occur along particular directions that might find their origin in the intrinsic astrophysics of the sources.

Keywords: Astrometry, Reference systems, Techniques: interferometric

1 Introduction

The International Celestial Reference Frame (ICRF3, Charlot et al. in prep.) is based on 4536 radio sources which are associated with Active Galactic Nuclei (AGN, Padovani et al. 2017). Those sources have been observed with Very Long Baseline Interferometry (VLBI) in its geodetic mode since 1979 in S/X (2GHz/8GHz) bands. In geodetic mode, the technique measures the source positions on the sky with an uncertainty which ranges from $30 \mu\text{as}$ to 1 mas or more, depending mostly on the number of times the source has been observed, from a few times to more than a thousand times. Given their cosmological distances, the detection of the proper motion of those sources is unreachable at these accuracies, and furthermore, they are compact on VLBI scales*. It is for all these reasons that these sources are well suited to realise the ICRF.

Since the first ICRF realisation in 1998 (Ma et al. 1998), it has been known however that some sources amongst the extensively observed ones show noticeable variations in their coordinates over time. Hence, the sources observed for astrometric and/or geodetic purposes are not always ideal fiducial marks on the sky, and it is necessary to select a set of primary sources, amongst the most stable ones, to define the fundamental axes of the frame at best. For the ICRF3, there are 303 such defining sources. Together, they ensure the axis stability of ICRF3 at the order of $10 \mu\text{as}$ (Charlot et al. in prep.).

Ten years ago, the number of very “unstable” sources (called special handling sources) was found to be 39, which is a small proportion[†] considering the 3414 sources of the whole ICRF2 (Fey et al. 2015). Recently, we have assessed the individual source stability, in an astrometric point of view, i.e. how much the source position varies. The next section describes the methodology used to this end and reports about the results (details are reported in Gattano et al. 2018).

2 Analysis of source astrometric behaviour

We used the observations from 24-hour sessions publicly available in the data centres of the International VLBI Service for astrometry and geodesy (IVS, Nothnagel et al. 2017) until august 2018. We computed the coordinate times series of 663 sources observed in more than 20 VLBI sessions (see Fig. 1 on the left for an

¹ Laboratoire d’astrophysique de Bordeaux, Univ. Bordeaux, CNRS, B18N, allée Geoffroy Saint-Hilaire, 33615 Pessac, France.

*VLBI images of a number of sources used to define the ICRF are available from the Bordeaux VLBI Image Database (BVID, Collioud & Charlot 2019) → <http://bvid.astrophy.u-bordeaux.fr/database.html>.

[†]Mainly due to the fact that most of the sources have not been observed enough to assess their coordinate variability.

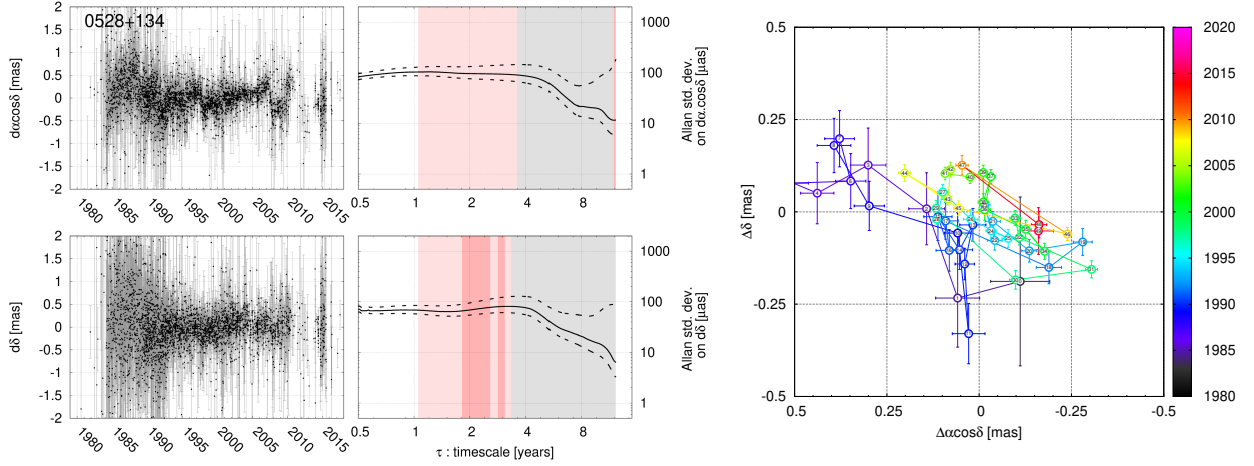


Fig. 1. Left: Coordinate time series of the source 0528+134 presented as right ascension (top) and declination (bottom) offsets with respect to the mean position of the source. Aside is the corresponding Allan standard deviation functions. They are given in a log-log scale with respect to the time scale, i.e. the length of the window used to compute the averaged positions of the source. A gray background indicates a stable position at the corresponding time scales, a red background indicates an unstable position, and a pink background indicates an intermediate phase. **Right:** Projection of the two coordinate times series (reduced to a few tens of points) trajectory on the sky plane.

example of the coordinate time series of a source observed several hundreds of times). Then, we analysed those time series using the Allan standard deviation, a statistical tool developed originally in the field of time metrology to analyse the stability of atomic clocks (Allan 1966). This tool enables (1) to estimate the standard deviation of the position at different time scales and (2) to distinguish the stability of the position (of which the measurements are considered as resulting from noise processes) at each of these time scales. The position stability is qualified from the slope of the Allan standard deviation function with respect to the time scale in a log-log representation (see Fig. 1). If the slope is negative, the position is defined as stable at the considered time scale in the sense that, if we pursue the observation of the considered source further (and access longer time scales), the position uncertainty will be improved (the time scale ranges associated with position stability are shown by a grey background in Fig. 1). An example is given by a purely white noise process, characterized with a slope equal to -0.5 . If the slope is positive, the position is defined as unstable at the considered time scale with an uncertainty degrading as the time scale increases (the time scale ranges associated with instability are shown by a red background in Fig. 1). For example, in the case of a purely red noise process, also called random walk, the slope is $+0.5$. The boundary in between is given by the pink noise process, also called flicker noise, which provides a position uncertainty that remains constant as the observations of the source accumulate.

We introduced as the source *astrometric behaviour* the sequence of the time scale dependent position stability considering the time scales starting from 1 year and increasing. For example, the declination of the source in Fig. 1 is characterized by a sequence “unstable (1–3 yrs) – stable (3–10 yrs)”. The astrometric behaviour is defined as stable in absence of instability in such a sequence. It is defined as unstable if instability is found on the longest time scales. Otherwise, it falls into an intermediate category. In practice, the two source coordinate time series were treated independently and we kept the worst category to decide upon the astrometric behaviour which qualify the source stability. A global indicator is also computed to quantify the source position stability based on the level of the source coordinate Allan standard deviation functions.

Figure 2 provides the results for our entire sample of 663 sources. By strictly applying the process above, the source sample counts 57 stable sources (designated AV0 sources), 160 unstable sources (designated AV2 sources) and 446 intermediate sources (designated AV1 sources). We further developed a statistical validation process based on a Monte-Carlo simulation of pure white noise signals sampled on the source observation epochs. This process enables the rehabilitation of AV2 and AV1 sources into AV1 or AV0 categories under the argument that a change of slope may originated from the irregularity of the sampling. It is based on the analysis of the spread

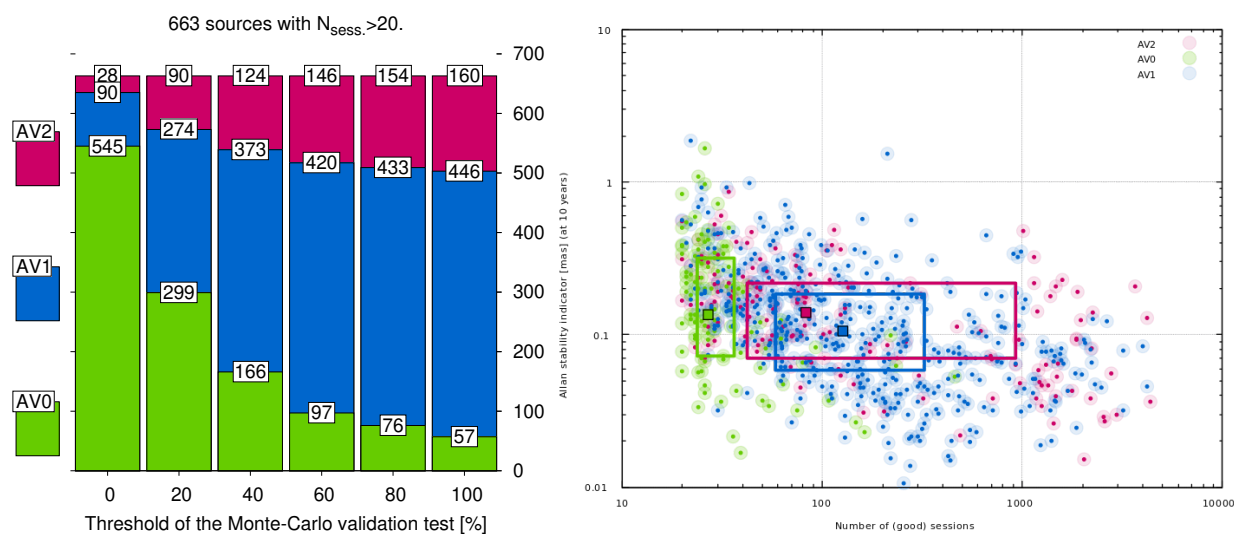


Fig. 2. Left: Source categorization depending on astrometric behaviour : stable (AV0, green), intermediate (AV1, blue), unstable (AV2, red). The percentage in abscissa indicates the threshold of a statistical validation test dealing with the trend of the computed Allan standard deviation functions. It enables rehabilitation for an increasing number of AV2 sources into AV1 or AV0 categories and AV1 sources into AV0 category when loosening the threshold (see text for details). **Right:** Distribution of the sources (categorized using a threshold at 60%, i.e. corresponding to the third bar from the right side of the left figure) according to the number of sessions in which they are observed and their position stability indicator based on the coordinate Allan standard deviation function. Filled squares indicate the median position for each category while the larger empty rectangles indicate the associated inner quartiles boundaries.

of simulated purely white noise Allan standard deviation functions which is due to this irregularity[‡] and how the source Allan standard deviation functions compare with this spread. The different bars on the left panel of Fig. 2 indicate the evolution of the categorization as the threshold of the rehabilitation is loosened. As shown in this graph, the threshold needs to be quite loosened to get a significantly different distribution. The right part of Fig. 2 presents the distribution of the sources (as categorized with the threshold fixed at 60%) with respect to the number of sessions in which they were observed and their source stability indicator. This distribution reveals that the stable sources are in majority the less observed sources. Our interpretation is that the accuracy of the astrometric VLBI technique is now such that all sources may show position instabilities if observed long enough.

Given this astrometric variability, nearly generalised to all the sources, we investigated in a second stage if the variation arises in random or peculiar source-dependent directions. The next section presents approach used and the results of this study.

3 Preferred directions for source astrometric variations

For the 215 sources observed more than 200 times, we attempted to extract preferred directions from the observed astrometric variations. We worked with reduced coordinate times series (i.e. with coordinates averaged every 50–100 observations) as shown for example in the right part of Fig. 1. Each successive pair of points was converted into a vector that provides the direction of the position variation between the two epochs. Coordinate uncertainties were converted in the direction uncertainty. Then, each vector direction was weighted with its normalized length and all directions and their uncertainties were combined to derive a Probability Density Function (PDF) characterizing the distribution of directions. From this PDF, the preferred direction and its uncertainty are then extracted from the peak of the PDF and its width, respectively. For some sources, two (or more) peaks show up, indicating that the variation arises in multiple preferred directions.

[‡]In the case of a regular sampling, a pure white noise signal provides a slope of -0.5 for the Allan standard deviation function in a log-log scale.

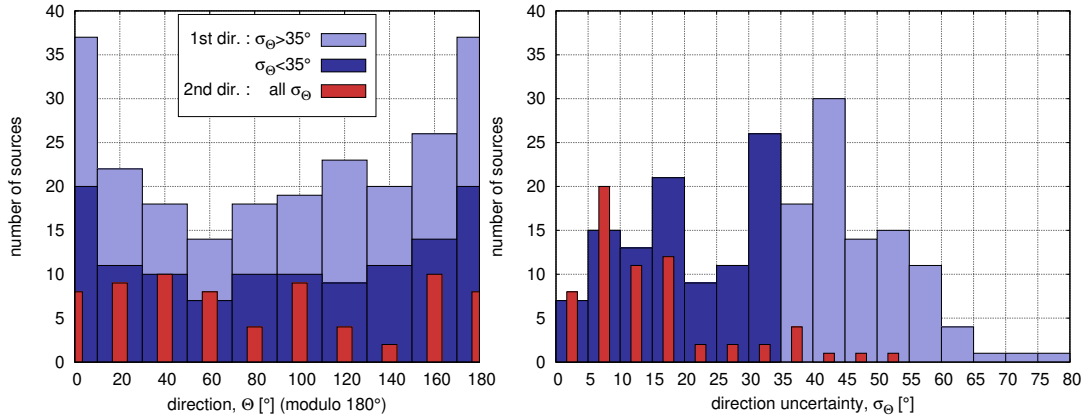


Fig. 3. Left: Distribution of the directions extracted from the source astrometric variations. In blue are presented the primary directions (successfully extracted for 90% of the sources), and in red the secondary directions (which are found for 30% of the sources). **Right:** Distribution of the direction uncertainties. Dark blue colour indicates well-constrained directions, i.e. with an uncertainty lower than 35° , while light blue colour indicates the directions that are not well-constrained, i.e. with an uncertainty larger than 35° .

Considering our sample, it is found that the astrometric variation arises in one (and only one) preferred direction for about 60% of the sources while for another 30%, it arises in two preferred directions. Figure 3 presents the distribution of those directions in the range 0° – 180° . The uncertainties are up to 80° . In this regard, we consider that a direction is well constrained if its uncertainty is lower than 35° . For the primary directions, the population is divided in two similar halves with about the same number of sources that have well-constrained directions and less constrained directions. On the opposite, the secondary directions are in majority well-constrained.

We note a peculiar excess of primary directions near 0° which corresponds to the north-south direction. It is known that the VLBI antenna network suffers for a lack of baselines oriented in this particular direction. This deficiency in the network induces a generally lower declination precision and potential systematics compared to the right ascension accuracy which may explain the excess of primary direction near 0° . On the contrary, the distribution of the rest of the sample is homogeneous and hence possibly indicates in that the astrometric variations originate from source intrinsic astrophysical phenomena. Finally, we note that the distribution of the secondary directions found for 30% of the sources does not show any particular excess.

4 Discussion and conclusion

In conclusion, the sources observed with geodetic VLBI and used to define the ICRF often show variations in their coordinates that limit their potential as ultra-accurate fiducial marks on the sky. Such source-dependent variations arise preferably in a particular direction, and occasionally in two different directions.

By observing AGN with VLBI, we focus on a small part of the source jet with a relatively compact structure. Nevertheless, this structure may be variable. It can become extended, or even split into one VLBI core and separate knots potentially moving down the jet, with the direction of the extension or the direction joining the VLBI core and the knots representing the direction of the source jet projected on the sky plane. A change of the source structure induces a variation of the VLBI delays depending on the relative orientation of this structure with respect to the projected observing baselines. Without correcting for such effect, the measured astrometric position of the source may thus vary without any true changes of the coordinates of its VLBI core.

Additionally, the VLBI core position may change as well. For example, if the jet is precessing, the VLBI core may follow an elliptical trajectory as projected on the sky. It is also suspected that the VLBI core could be subjected to position instability along the jet, shifted downstream and upstream, due to occasional burst of the AGN activity. Finally, the presence of two (or more) supermassive black holes orbiting around each, each possibly having a variable VLBI core, may further complicate the picture. In this case the astrometric position measured with VLBI may be switched between the locations of the different VLBI cores depending on which one is brighter at a given time.

Observations of the ICRF3 sources continue. As time goes, these will keep bringing new information for a

better understanding of the astrometric position variations, and hence of the underlying source physics. All such information will also contribute to adapting our strategies for the scheduling of the observations and further improve the realisation of the celestial reference frame.

This work has been supported by a CNES post-doctoral grant. These studies use data and products from the International VLBI Service for astrometry and geodesy.

References

- Allan, D. W. 1966, IEEE Proceedings, 54, 221
- Charlot, P., Jacobs, C. S., Gordon, D., et al. in prep., A&A
- Collioud, A. & Charlot, P. 2019, in Proceedings of the 24th meeting of the European VLBI group for Geodesy and Astrometry
- Fey, A. L., Gordon, D., Jacobs, C. S., et al. 2015, AJ, 150, 58
- Gattano, C., Lambert, S. B., & Le Bail, K. 2018, A&A, 618, A80
- Ma, C., Arias, E. F., Eubanks, T. M., et al. 1998, AJ, 116, 516
- Nothnagel, A., Artz, T., Behrend, D., & Malkin, Z. 2017, Journal of Geodesy, 91, 711
- Padovani, P., Alexander, D. M., Assef, R. J., et al. 2017, Astronomy and Astrophysics Review, 25, 2